GRSL-00503-2023.R2

Stage 1 Validation of Plant Area Index from the Global Ecosystem Dynamics Investigation

Luke A. Brown, Harry Morris, Courtney Meier, Alexander Knohl, Christian Lanconelli, Nadine Gobron, Jadunandan Dash and F. Mark Danson

***Abstract*—The Global Ecosystem Dynamics Investigation (GEDI) aims to provide improved characterization of forest structure, and plant area index (PAI) is one of many variables provided in the official GEDI Level 2B (L2B) product suite. However, since release, few quantitative validation studies have been conducted. To reach Stage 1 of the validation hierarchy proposed by the Land Product Validation (LPV) sub-group of the Committee on Earth Observation Satellites (CEOS) Working Group on Calibration and Validation (WGCV), we provide an initial assessment of PAI estimates from GEDI's L2B product. This is achieved using 18 in situ reference measurements available through the Copernicus Ground Based Observations for Validation (GBOV) service. We show that GEDI L2B PAI retrievals provide a nearly unbiased estimate of effective (PAI_e) (RMSD = 0.95, bias = 0.02, slope = 1.07), but systematically underestimate PAI (RMSD = 1.42, bias = -0.91, slope = 0.77). This is attributed to an assumed random distribution of plant material in the algorithm. To reach Stage 2 of the CEOS WGCV LPV hierarchy, continued work is needed to validate the product against additional in situ reference measurements covering further locations and time periods.**

This activity was carried out under the Living Planet Fellowship, a programme of and funded by the European Space Agency. The view expressed in this publication can in no way be taken to reflect the official opinion of the European Space Agency. This study has been undertaken using data from GBOV 'Ground Based Observations for Validation' (https://land.copernicus.eu/global/gbov) funded by the European Commission Joint Research Centre FWC 932059, part of the Global Component of the European Union's Copernicus Land Monitoring Service. The National Ecological Observatory Network is a program sponsored by the National Science Foundation and operated under cooperative agreement by Battelle. This material is based in part upon work supported by the National Science Foundation through the NEON Program. *(Corresponding author: Luke A. Brown).*

Luke A. Brown and F. Mark Danson are with the School of Science, Engineering & Environment, University of Salford, Manchester, M5 4WT, United Kingdom (e-mail: l.a.brown4@salford.ac.uk, f.m.danson@salford.ac.uk).

Harry Morris is with the Earth Observation, Climate and Optical Group, National Physical Laboratory, Teddington, TW11 0LW, United Kingdom (e-mail: harry.morris@npl.co.uk).

Courtney Meier is with the National Ecological Observatory Network, Battelle, Boulder, CO 80301, United States (e-mail: cmeier@battelleecology.org).

Alexander Knohl is with the Department of Bioclimatology, University of Göttingen, 37077 Göttingen, Germany (e-mail: aknohl@gwdg.de).

Christian Lanconelli is with UniSystems, 20145 Milan, Italy (e-mail: christian.lanconelli@ext.ec.europa.eu).

Nadine Gobron is with the European Commission Joint Research Centre, 21027 Ispra, Italy (e-mail: nadine.gobron@ec.europa.eu).

Jadunandan Dash is with the School of Geography and Environmental Science, University of Southampton, Highfield, Southampton, SO17 1BJ, United Kingdom (e-mail: j.dash@soton.ac.uk).

Color versions of one or more of the figures in this article are available online at http://ieeexplore.ieee.org

***Index Terms*—Ground Based Observations for Validation (GBOV), GEDI, leaf area index (LAI), PAI**

I. INTRODUCTION

THE Global Ecosystem Dynamics Investigation (GEDI) was installed on-board the International Space Station (ISS) in 2018, with the aim of providing higher quality characterization of the structure of the world's temperate and tropical forests than previously possible [1]. Based upon full-waveform light detection and ranging (LiDAR), GEDI builds upon the heritage of the Ice, Cloud and Land Elevation Satellite (ICESat) missions, whose Geoscience Laser Altimeter System (GLAS) and Advanced Topographic Laser Altimeter System (ATLAS) instruments have already proven useful for characterizing forest structure [2]–[5].

Key variables describing the structure of forest canopies include plant area index (PAI) and leaf area index (LAI), which are unitless quantities representing half the unit surface area of plant or leaf material per unit horizontal ground area, respectively [6]. By regulating the size of the interface between the biosphere and atmosphere, PAI and LAI determine the interception of light and exert control on photosynthesis and plant respiration. Thus, they are critical variables for modelling vegetation productivity, carbon exchange, and the weather and climate systems [7], [8]. More broadly, as indicators of the density of the canopy, they represent useful metrics for monitoring forest condition.

Using spaceborne passive optical instruments, a range of LAI and PAI products have emerged over the last twenty years, making use of radiative transfer models (RTMs) to link observed canopy spectral properties to the structural variables of interest [9]–[13]. The key issues with these products are that the adopted RTMs make simplifying assumptions about the canopy [14], [15], and that RTM inversion is ill-posed, in that multiple combinations of input parameters can result in similar spectral properties, confounding retrieval [15]–[17]. Although still subject to the ill-posed nature of the inverse problem, unlike passive optical instruments, active LiDAR instruments such as GLAS, ATLAS, and GEDI can be considered to provide a more direct measurement of canopy structure. As such, they are well-placed to minimize these sources of uncertainty.

Early work using GLAS and ATLAS data investigated the feasibility of estimating LAI and PAI with spaceborne LiDAR. These studies demonstrated that good retrieval accuracies were achievable (r^2 > 0.80, RMSE < 0.50). In particular, the spaceborne LiDAR derived estimates demonstrated reduced bias compared to products derived from passive optical instruments, and were not subject to saturation at high LAI and PAI values [2]–[4]. Despite their potential for LAI and PAI estimation, however, the real-world utility of early spaceborne LiDAR instruments such as GLAS and ATLAS was severely limited by their sparse spatial sampling (i.e. GLAS sampled 70 m footprints every 170 m along a single track) [1]. By contrast, GEDI offers substantially increased sampling density (25 m footprints sampled every 60 m along eight parallel tracks 600 m apart).

Based upon the success of early studies using GLAS and ATLAS, PAI is one of many variables provided in the official GEDI Level 2B (L2B) product suite. Since release, however, few quantitative validation studies using in situ reference measurements have been conducted [18]. Validation against independent in situ reference measurements is essential to ensure fitness-for-purpose. The objective of this letter, therefore, is to provide an initial assessment of the accuracy of PAI estimates from GEDI's L2B product. In doing so, we aim to reach Stage 1 of the validation hierarchy proposed by the Land Product Validation (LPV) sub-group of the Committee on Earth Observation Satellites (CEOS) Working Group on Calibration and Validation (WGCV), which states that 'product accuracy is assessed from a small (typically < 30) set of locations and time periods by comparison with in situ or other suitable reference data' [19]. It is worth noting that because GEDI's PAI retrievals do not consider clumping, they correspond to effective PAI (PAI_e). As such, we hypothesize that better agreement with in situ reference measurements of PAI_e as opposed to PAI will be observed.

II. Materials and Methods

A. GEDI Data

GEDI L2B PAI data were obtained from the 'LARSE/GEDI/GEDI02_B_002_MONTHLY' collection in Google Earth Engine [20], which represents rasterized monthly composites of the original L2B vector dataset. It is worth noting that unlike the L3 product, the rasterized L2B data remain at the footprint level, and are not spatially interpolated (i.e. 25 m pixels representing a single GEDI footprint contain data, whilst surrounding pixels contain no data). The provided quality flags were used to restrict our analysis to observations meeting criteria on energy, sensitivity, amplitude, real-time surface tracking quality, and difference to a digital elevation model (i.e. L2B quality flag = 1 and L2A degrade flag = 0).

B. In Situ Reference Measurements

In situ reference measurements were obtained from the Copernicus Ground Based Observations for Validation (GBOV) service, as previously described in [21], [22]. Data matching GEDI observations were available at ten sites belonging to the National Ecological Observatory Network (NEON) in the United States [23], and a further site affiliated to the Integrated Carbon Observation System (ICOS) in Europe [24]. The latter site, Hainich National Park, in Germany, was set up as a permanently instrumented site under Component 2 of GBOV [25]. These sites covered a range of vegetation types, including deciduous forest, evergreen forest, grassland/herbaceous vegetation, pasture/hay, shrub/scrub, and woody wetlands (Table I).

TABLE I
SITES AT WHICH IN SITU REFERENCE MEASUREMENTS WERE OBTAINED

Site	Network	Land cover type	Latitude	Longitude	Canopy height (m)	Valid matchups	Range of in situ PAI_e (and PAI)
Blandy Experimental Farm	NEON	Deciduous forest	39.0603	-78.0716	1.0	2	1.4 to 3.4 (1.5 to 4.9)
Central Plains Experimental Range	NEON	Grassland /herbaceous	40.8155	-104.7460	0.4	1	< 0.1
Dead Lake	NEON	Deciduous forest	32.5417	-87.8039	30.0	2	3.5 to 4.2 (4.7 to 5.6)
Disney Wilderness Preserve	NEON	Pasture /hay	28.1250	-81.4362	1.5	1	0.4 (0.4)
Hainich National Park	ICOS	Deciduous forest	51.0794	10.4532	35.0	3	3.4 to 5.9 (4.9 to 7.7)
Jones Ecological Research Center	NEON	Evergreen forest	31.1948	-84.4686	27.0	1	1.7 (2.3)
Onaqui	NEON	Shrub /scrub	40.1776	-112.4520	1.2	1	< 0.1
Oak Ridge	NEON	Deciduous forest	35.9641	-84.2826	28.0	1	0.6 (0.8)
Talladega National Forest	NEON	Evergreen forest	32.9505	-87.3933	25.0	3	1.0 to 1.4 (1.3 to 2.1)
UNDERC	NEON	Woody wetlands	46.2339	-89.5373	24.0	3	3.6 to 3.8 (5.2 to 5.7)

Note that the GEDI L2B product separates the returned waveform into bins of 5 m. PAI retrievals for canopies shorter than 5 m are, therefore, expected to be less reliable. By incorporating several sites with short canopies, it was our explicit intention to test this. In the absence of a quality flag to filter out such observations, information on the potential magnitude of errors will likely prove useful to users.

At each site, in situ reference measurements were acquired using digital hemispherical photography (DHP) and processed with HemiPy [26], as adopted by the GBOV service, using default settings. At NEON sites, images were acquired in both upwards- and downwards-facing directions using a Nikon D750, D800 or D810 digital single lens reflex (DSLR) camera equipped with an AF Fisheye-Nikkor 16mm f/2.8D full-frame fisheye lens. At Hainich National Park, images were acquired using a Canon EOS 750D or 1300D DSLR equipped with a Sigma 4.5 mm F2.8 EX DC circular fisheye lens. In both cases, images were obtained within elementary sampling units (ESUs) of between 20 m x 20 m and 40 m x 40 m. Twelve replicates were performed in a cross pattern at NEON sites [27], whilst thirteen were performed for manual DHP acquisitions at Hainich National Park [25].

PAI and PAI_e were derived according to [28] and [29], making using of gap fraction observations at the hinge angle of 57.5° (± 5°), such that

$$PAI = \frac{-\overline{\ln P(\theta_{57.5°})}}{0.93} \tag{1}$$

$$PAI_e = \frac{-\ln \overline{P(\theta_{57.5°})}}{0.93} \quad (2)$$

where $\overline{\ln P(\theta_{57.5°})}$ represents the mean of the natural logarithm of gap fraction values within a zenith ring centered at 57.5° (± 5°) over all azimuth cells and images, whilst $\ln \overline{P(\theta_{57.5°})}$ represents the natural logarithm of the mean gap fraction value within the same zenith ring.

Values from upwards- and downwards-facing images were combined to provide a total value, such that

$$PAI = PAI_{up} + PAI_{down} \quad (3)$$

where PAI_{up} and PAI_{down} represent PAI or PAI_e values derived from upwards- and downwards-facing images, respectively. Uncertainties were computed following Fiducial Reference Measurements for Vegetation (FRM4VEG) guidelines [30], accounting for variability in gap fraction and uncertainty due to camera levelling.

C. Spatiotemporal Matchup Procedure and Statistical Analysis

Valid GEDI L2B PAI observations were matched to in situ reference measurements whose footprint they fell within. The maximum in situ reference measurement within each monthly compositing period was used for comparison. This strategy attempts to reduce the impact of errors in the in situ measurements, and assumes noise in the DHP data is negatively biased (as previously demonstrated for automated DHP in the case of suboptimal illumination conditions [31]). The footprint of the in situ reference measurements was approximated according to [21] as

$$2\,h\,\tan(\theta) + l \quad (4)$$

where h represents the distance from the camera lens to the top (or bottom) of the canopy, θ represents the zenith angle analyzed, and l represents the one-sided length of the ESU. The mean of all valid GEDI L2B observations within the footprint was computed (Fig. 1).

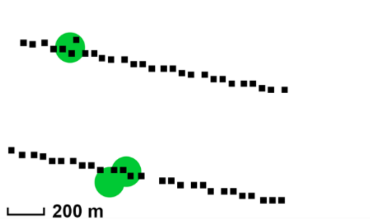

Fig. 1. Illustration of the footprint matching procedure over Hainich National Park (canopy height = 35 m, in situ reference measurement footprint = 145 m) for two GEDI tracks. The mean of all valid GEDI L2B PAI observations (black squares) intersecting the footprint of each in situ reference measurement (green circles) was calculated.

To assess the agreement between the GEDI L2B observations and in situ reference measurements, several statistics were calculated, including the slope, intercept, and coefficient of determination (r^2) according to ordinary least squares regression. Additionally, we calculated the root mean square difference (RMSD), normalized RMSD (i.e. RMSD divided by the mean of the in situ reference measurements), minimum and maximum difference, bias (i.e. mean difference), precision (i.e. standard deviation of differences), and uncertainty agreement ratio (UAR). The UAR corresponded to the percentage of retrievals falling within the Sentinels for Science (SEN4SCI) uncertainty requirements of 1 unit or 20% [22], [32], [33].

III. Results

A. Characteristics of In Situ Reference Measurements and GEDI L2B PAI data

A total of 18 GEDI L2B PAI estimates were spatiotemporally coincident with the in situ reference measurements described in Section II. GEDI L2B PAI values ranged from 0.00 to 5.23, with a mean of 2.42, whilst the corresponding in situ reference measurements of PAI_e ranged from 0.00 to 5.94, with a mean of 2.40 (Fig. 2). In contrast, the corresponding in situ reference measurements of PAI demonstrated a greater range (0.00 to 7.70) and were higher on average (mean = 3.33) (Fig. 2).

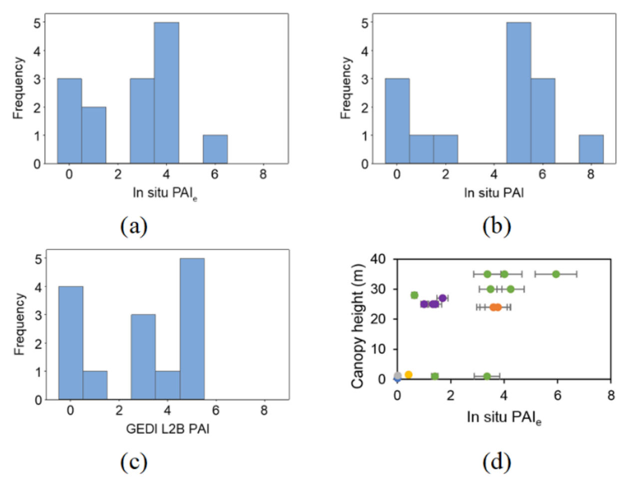

Fig. 2. Frequency distribution of in situ reference measurements of PAI_e (a) and PAI (b), in addition to frequency distribution of GEDI L2B PAI values (c), and comparison of in situ PAI_e against canopy height (d). Please refer to Fig. 3 for interpretation of the colours in (d).

B. Validation Results

When analyzed on a pairwise basis, the GEDI L2B PAI estimates had substantially better agreement with in situ reference measurements of PAI_e than with in situ reference measurements of PAI. This was demonstrated by a reduced RMSD (0.95 for PAI_e as opposed to 1.42 for PAI) and NRMSD (40% for PAI_e as opposed to 43% for PAI), increased UAR (67% for PAI_e as opposed to 50% for PAI) (Table II), and by points lying closer to the 1:1 line in the case of PAI_e than in the case of PAI (Fig. 3). GEDI L2B PAI retrievals provided a nearly unbiased estimate of in situ reference PAI_e (bias = 0.02, slope = 1.07), but systematically underestimated in situ reference PAI (bias = -0.91, slope = 0.77) (Table II).

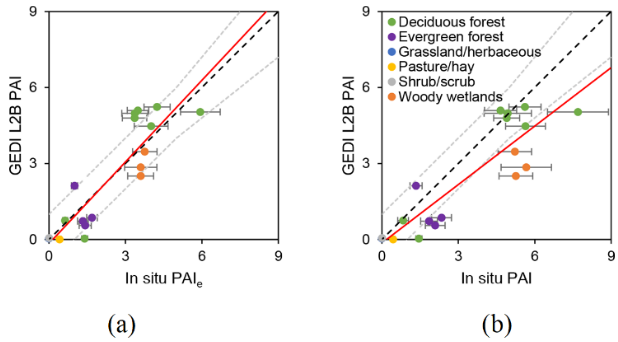

Fig. 3. Scatterplots of GEDI L2B PAI and in situ reference measurements of PAI_e (a) and PAI (b). Dashed lines represent a 1:1 relationship, dotted lines represent SEN4SCI uncertainty requirements, and error bars represent the expanded uncertainty of the in situ reference measurements at a coverage factor (k) of 3 (i.e. a ~ 99% confidence interval).

TABLE II
VALIDATION METRICS FOR GEDI L2B PAI WITH RESPECT TO IN SITU REFERENCE MEASUREMENTS OF PAI_E AND PAI

Statistic	PAI_e	PAI
r^2	0.78	0.78
Slope	1.07	0.77
Intercept	-0.16	-0.14
RMSD	0.95	1.42
NRMSD (%)	39.50	42.51
Minimum difference	-1.37	-2.82
Maximum difference	1.61	0.78
Bias	0.02	-0.91
Precision	0.98	1.12
UAR (%)	66.67	50.00

IV. DISCUSSION AND CONCLUSION

Relatively few studies have attempted to directly validate estimates of PAI from spaceborne LiDAR instruments against in situ reference measurements, with most studies relying on reference PAI values derived from airborne LiDAR or passive optical imagery. Exceptions include [4], who developed and validated an empirical model relating GLAS observations to in situ reference PAI_e measurements from the LI-COR LAI-2000 over a study site in the Tibetan Plateau, as well as [3] and [34], who developed physically-based PAI_e and PAI retrieval approaches for GLAS data, validating them against in situ reference measurements using the Tracing Radiation Architecture of Canopies (TRAC) instrument in Heilojiang Province and the Tibetan Plateau, respectively. Our results are consistent with these studies, which reported better agreement with in situ reference measurements of PAI_e (r^2 = 0.79 to 0.85, RMSD = 0.31 to 0.49) than PAI (r^2 = 0.74, RMSD = 1.18).

Given that GEDI L2B PAI estimates assume a random distribution of plant material (i.e. no clumping), the closer agreement with in situ reference measurements of PAI_e as opposed to PAI is not unexpected. Since the bias with respect to in situ reference measurements appeared to be quite systematic for each vegetation type, it is possible that land cover based bias corrections could be applied to correct the GEDI L2B PAI estimates, though more data would be needed to confirm this possibility.

Whilst only a limited number of in situ reference measurements were available with which to validate the GEDI L2B PAI product, it is encouraging that from these measurements, GEDI L2B PAI retrievals appear to provide a nearly unbiased estimate of PAI_e. Nevertheless, it should be noted that for the deciduous forest and woody wetlands sites where PAI_e > 3, GEDI observations were characterized by substantial range that was not observed in the in situ reference measurements. Although this could be symptomatic of an issue in the GEDI data, it could equally result from the various sources of uncertainty that our results are subject to, including those associated with the in situ reference measurements themselves, the method used to approximate their footprint, and the spatiotemporal mismatch between the in situ reference measurements and GEDI observations. In future work, the latter source of uncertainty could be better understood by investigating sensitivity to the number of GEDI observations averaged (where multiple GEDI observations fall within an in situ reference measurement's footprint).

Although spaceborne LiDAR instruments such as GEDI cannot yet provide the same spatiotemporal coverage as passive optical instruments, they could prove a useful source of information for calibration and validation of products derived from these latter instruments, providing an independent measurement of PAI_e that is more directly related to canopy structure. Given that the spatial resolution of imagers on-board missions such as Sentinel-2 (20 m) and Landsat 8/9 (30 m) is a close match to GEDI's 25 m footprint, future work should focus on intercomparison of the GEDI L2B PAI product with biophysical variable retrievals from these missions, including those derived using the Sentinel-2 Level 2 Prototype Processor (SL2P) [22], [33].

As a result of the uncertainties in our study, continued work is needed to validate the GEDI L2B PAI product against additional in situ reference measurements covering further locations and time periods, with a particular focus on the 2 m to 24 m height range that was not well represented by our data (Fig. 2d). Indeed, Stage 2 of the CEOS WGCV LPV hierarchy requires that validation is carried out at over at least 30 locations and time periods. In addition to dedicated field campaigns, efforts should be placed on leveraging existing in situ reference datasets that cover the mission's lifetime. For example, although NEON collects DHP at 47 sites, only data from 24 of these sites have been processed and are available under the GBOV service so far. Routine data collected by networks such as ICOS, the Terrestrial Ecosystem Research Network (TERN) in Australia [35], and the Chinese Ecosystem Research Network (CERN) [36] should also be investigated to increase the number of spatiotemporal matchups available for validation.

ACKNOWLEDGEMENT

The authors are grateful to Frank Tiedemann for field assistance and instrument maintenance at Hainich National Park.

REFERENCES

[1] R. Dubayah et al., "The Global Ecosystem Dynamics Investigation: High-resolution laser ranging of the Earth's forests and topography," Sci. Remote Sens., vol. 1, no. September 2019, p. 100002, Jun. 2020, doi: 10.1016/j.srs.2020.100002.

[2] H. Tang, R. Dubayah, M. Brolly, S. Ganguly, and G. Zhang, "Large-scale retrieval of leaf area index and vertical foliage profile from the spaceborne waveform lidar (GLAS/ICESat)," Remote Sens. Environ., vol. 154, pp. 8–18, Nov. 2014, doi: 10.1016/j.rse.2014.08.007.

[3] L. Cui et al., "Retrieval of Vertical Foliage Profile and Leaf Area Index Using Transmitted Energy Information Derived from ICESat GLAS Data," Remote Sens., vol. 12, no. 15, p. 2457, Jul. 2020, doi: 10.3390/rs12152457.

[4] S. Luo, C. Wang, G. Li, and X. Xi, "Retrieving leaf area index using ICESat/GLAS full-waveform data," Remote Sens. Lett., vol. 4, no. 8, pp. 745–753, Aug. 2013, doi: 10.1080/2150704X.2013.790573.

[5] J. Zhang et al., "Leaf area index retrieval with ICESat-2 photon counting LiDAR," Int. J. Appl. Earth Obs. Geoinf., vol. 103, p. 102488, Dec. 2021, doi: 10.1016/j.jag.2021.102488.

[6] J. M. Chen and T. A. Black, "Measuring leaf area index of plant canopies with branch architecture," Agric. For. Meteorol., vol. 57, no. 1–3, pp. 1–12, Dec. 1991, doi: 10.1016/0168-1923(91)90074-Z.

[7] A. D. Richardson, T. F. Keenan, M. Migliavacca, Y. Ryu, O. Sonnentag, and M. Toomey, "Climate change, phenology, and phenological control of vegetation feedbacks to the climate system," Agric. For. Meteorol., vol. 169, pp. 156–173, Feb. 2013, doi: 10.1016/j.agrformet.2012.09.012.

[8] P. J. Sellers et al., "Modeling the Exchanges of Energy, Water, and Carbon Between Continents and the Atmosphere," Science (80-.)., vol. 275, no. 5299, pp. 502–9, Jan. 1997, doi: 10.1126/science.275.5299.502.

[9] K. Yan et al., "Evaluation of MODIS LAI/FPAR Product Collection 6. Part 2: Validation and Intercomparison," Remote Sens., vol. 8, no. 6, p. 460, May 2016, doi: 10.3390/rs8060460.

[10] K. Yan et al., "Generating Global Products of LAI and FPAR From SNPP-VIIRS Data: Theoretical Background and Implementation," IEEE Trans. Geosci. Remote Sens., vol. 56, no. 4, pp. 2119–2137, Apr. 2018, doi: 10.1109/TGRS.2017.2775247.

[11] B. Pinty et al., "Exploiting the MODIS albedos with the Two-stream Inversion Package (JRC-TIP): 1. Effective leaf area index, vegetation, and soil properties," J. Geophys. Res., vol. 116, no. D9, p. D09105, May 2011, doi: 10.1029/2010JD015372.

[12] F. J. García-Haro et al., "Climate Data Records of Vegetation Variables from Geostationary SEVIRI/MSG Data: Products, Algorithms and Applications," Remote Sens., vol. 11, no. 18, p. 2103, Sep. 2019, doi: 10.3390/rs11182103.

[13] H. Fang, F. Baret, S. Plummer, and G. Schaepman-Strub, "An Overview of Global Leaf Area Index (LAI): Methods, Products, Validation, and Applications," Rev. Geophys., vol. 57, no. 3, pp. 739–799, Sep. 2019, doi: 10.1029/2018RG000608.

[14] K. Richter, C. Atzberger, F. Vuolo, P. Weihs, and G. D'Urso, "Experimental assessment of the Sentinel-2 band setting for RTM-based LAI retrieval of sugar beet and maize," Can. J. Remote Sens., vol. 35, no. 3, pp. 230–247, Jan. 2009, doi: 10.5589/m09-010.

[15] A. Verger, F. Baret, and F. Camacho, "Optimal modalities for radiative transfer-neural network estimation of canopy biophysical characteristics: Evaluation over an agricultural area with CHRIS/PROBA observations," Remote Sens. Environ., vol. 115, no. 2, pp. 415–426, Feb. 2011, doi: 10.1016/j.rse.2010.09.012.

[16] B. Combal et al., "Retrieval of canopy biophysical variables from bidirectional reflectance," Remote Sens. Environ., vol. 84, no. 1, pp. 1–15, Jan. 2003, doi: 10.1016/S0034-4257(02)00035-4.

[17] J. Verrelst et al., "Optical remote sensing and the retrieval of terrestrial vegetation bio-geophysical properties – A review," ISPRS J. Photogramm. Remote Sens., vol. 108, pp. 273–290, Oct. 2015, doi: 10.1016/j.isprsjprs.2015.05.005.

[18] S. Dhargay, C. S. Lyell, T. P. Brown, A. Inbar, G. J. Sheridan, and P. N. J. Lane, "Performance of GEDI Space-Borne LiDAR for Quantifying Structural Variation in the Temperate Forests of South-Eastern Australia," Remote Sens., vol. 14, no. 15, p. 3615, Jul. 2022, doi: 10.3390/rs14153615.

[19] R. Fernandes et al., "Global Leaf Area Index Product Validation Good Practices," in Best Practice for Satellite-Derived Land Product Validation, 2.0., R. Fernandes, S. Plummer, and J. Nightingale, Eds. Land Product Validation Subgroup (Committee on Earth Observation Satellites Working Group on Calibration and Validation), 2014. doi: 10.5067/doc/ceoswgcv/lpv/lai.002.

[20] N. Gorelick, M. Hancher, M. Dixon, S. Ilyushchenko, D. Thau, and R. Moore, "Google Earth Engine: Planetary-scale geospatial analysis for everyone," Remote Sens. Environ., vol. 202, pp. 18–27, Dec. 2017, doi: 10.1016/j.rse.2017.06.031.

[21] L. A. Brown et al., "Evaluation of global leaf area index and fraction of absorbed photosynthetically active radiation products over North America using Copernicus Ground Based Observations for Validation data," Remote Sens. Environ., vol. 247, p. 111935, Sep. 2020, doi: 10.1016/j.rse.2020.111935.

[22] L. A. Brown et al., "Validation of baseline and modified Sentinel-2 Level 2 Prototype Processor leaf area index retrievals over the United States," ISPRS J. Photogramm. Remote Sens., vol. 175, no. February, pp. 71–87, May 2021, doi: 10.1016/j.isprsjprs.2021.02.020.

[23] R. H. Kao et al., "NEON terrestrial field observations: designing continental-scale, standardized sampling," Ecosphere, vol. 3, no. 12, p. art115, Dec. 2012, doi: 10.1890/ES12-00196.1.

[24] B. Gielen et al., "Ancillary vegetation measurements at ICOS ecosystem stations," Int. Agrophysics, vol. 32, no. 4, pp. 645–664, Dec. 2018, doi: 10.1515/intag-2017-0048.

[25] L. A. Brown et al., "Potential of Automated Digital Hemispherical Photography and Wireless Quantum Sensors for Routine Canopy Monitoring and Satellite Product Validation," in Proceedings of the 2021 IEEE International Geoscience and Remote Sensing Symposium, 2021, pp. 53–56. doi: 10.1109/IGARSS47720.2021.9553564.

[26] L. A. Brown et al., "HemiPy: A Python module for automated estimation of forest biophysical variables and uncertainties from digital hemispherical photographs," Methods Ecol. Evol., vol. 14, no. 9, pp. 2329-2340, Sep. 2023, doi: 10.1111/2041-210X.14199.

[27] C. Meier, J. Everhart, and K. Jones, TOS Protocol and Procedure: Measurement of Leaf Area Index, K. Boulder, Colorado, United States: National Ecological Observatory Network, 2018.

[28] J. Warren-Wilson, "Estimation of foliage denseness and foliage angle by inclined point quadrats," Aust. J. Bot., vol. 11, no. 1, pp. 95–105, 1963.

[29] A. R. G. Lang and X. Yueqin, "Estimation of leaf area index from transmission of direct sunlight in discontinuous canopies," Agric. For. Meteorol., vol. 37, no. 3, pp. 229–243, Aug. 1986, doi: 10.1016/0168-1923(86)90033-X.

[30] L. A. Brown et al., "Fiducial Reference Measurements for Vegetation Bio-Geophysical Variables: An End-to-End Uncertainty Evaluation Framework," Remote Sens., vol. 13, no. 16, p. 3194, Aug. 2021, doi: 10.3390/rs13163194.

[31] L. A. Brown, B.O. Ogutu, and J. Dash, "Tracking forest biophysical properties with automated digital repeat photography: A fisheye perspective using digital hemispherical photography from below the canopy", Agric. For. Meteorol. vol. 287, p. 107944, Jun. 2020, doi: 10.1016/j.agrformet.2020.107944.

[32] SEN4SCI, "Assessing product requirements for the scientific exploitation of the Sentinel missions," 2011. http://www.geo.uzh.ch/microsite/sen4sci/ (accessed Jan. 29, 2020).

[33] R. Fernandes et al., "Validation of Simplified Level 2 Prototype Processor Sentinel-2 fraction of canopy cover, fraction of absorbed photosynthetically active radiation and leaf area index products over North American forests," Remote Sens. Environ., vol. 293, no. December 2022, p. 113600, Aug. 2023, doi: 10.1016/j.rse.2023.113600.

[34] H. Jiang et al., "Correcting Crown-Level Clumping Effect for Improving Leaf Area Index Retrieval From Large-Footprint LiDAR: A Study Based on the Simulated Waveform and GLAS Data," IEEE J. Sel. Top. Appl. Earth Obs. Remote Sens., vol. 14, pp. 12386–12402, Nov. 2021, doi: 10.1109/JSTARS.2021.3130738.

[35] M. Karan et al., "The Australian SuperSite Network: A continental, long-term terrestrial ecosystem observatory," Sci. Total Environ., vol. 568, pp. 1263–1274, Oct. 2016, doi: 10.1016/j.scitotenv.2016.05.170.

[36] B. Fu et al., "Chinese ecosystem research network: Progress and perspectives," Ecol. Complex., vol. 7, no. 2, pp. 225–233, Jun. 2010, doi: 10.1016/j.ecocom.2010.02.007.